Journal of Alloys and Compounds 537 (2012) 50–53

Contents lists available at SciVerse ScienceDirect

Journal of Alloys and Compounds

journal homepage: www.elsevier.com/locate/jalcom

Facile synthesis and improved photoluminescence of periodic SiC nanorod arrays by SiO_2 templates-assisted magnetron sputtering method

Zhenyu Li [a], Dengteng Ge [a], Lili Yang [b], Xin Liu [a], Yanbo Ding [c], Lei Pan [a], Jiupeng Zhao [c], Yao Li [a,*]

[a] Center for Composite Materials and Structure, Harbin Institute of Technology, Harbin 150001, China
[b] School of Transportation Science and Engineering, Harbin Institute of Technology, Harbin 150090, China
[c] School of Chemical Engineering and Technology, Harbin Institute of Technology, Harbin 150001, China

ARTICLE INFO

Article history:
Received 14 April 2012
Received in revised form 17 May 2012
Accepted 18 May 2012
Available online 27 May 2012

Keywords:
SiC
Nanostructured materials
Photoluminescence
Scanning electron microscopy

ABSTRACT

Silicon carbide (SiC) nanorod arrays with closely-packed periodic architecture are successfully fabricated by magnetron sputtering using SiO_2 colloidal monolayer as template. The growth mechanism and photoluminescence (PL) characteristics of SiC nanorod arrays have been investigated. It is found that the arrays periodicity can easily be controlled by the different sizes of SiO_2 spheres. The arrays prepared from smaller SiO_2 spheres are prone to be densely integrated and top aggregation, while more defects and shorter periodicity are found for arrays from bigger spheres. Improved PL performance of SiC nanorod arrays is revealed with enhancement ratios proportion to the diameters of SiC nanorods, which is caused by their special light manipulating properties and greater surface areas. The enhanced PL of SiC nanorod arrays is highly promising for use in designing highly efficient optical devices.

1. Introduction

Nanostructured ordered arrays (e.g., nanorods and nanotubes) have recently attracted more and more interest due to their applications in magnetics, optics, electrical and thermal transport [1–3]. Great concern has been taken to fabricate nanostructured ordered arrays, and the main challenge is obtaining well controlled morphologies and structures. The most popular methods are conventional lithographies, including electron-beam lithography, photolithography, X-ray lithography and scanning tunneling microscopy. However their low productivity and high cost strongly restrict their wide applications for nanostructured arrays [4–6]. Anodic aluminum oxide (AAO) templates method has the advantages of low cost and good repetition, but the nanostructured particles without the support of AAO templates are prone to aggregate and even collapse which restrict their application in nanodevices [7,8]. Compared with mentioned methods, the monolayer colloidal crystal template method has been proved to be a promising technique due to its simplicity, high efficiency and low cost [9–11]. Therefore lots of attentions have been attracted to the monolayer colloidal crystal template technique to fabricate new hierarchical nanostructure.

SiC is a very important functional material for photocatalysis, high-temperature and high-power devices, optical materials and high-speed devices [12–14]. However, the low light emission efficiency caused by indirect band gap structure has limited its applications in optoelectronic devices. Recently, several hierarchical SiO_2/SiC nanostructures, such as two-dimension SiO_2/SiC films, SiC/SiO_2 nanocables and SiC/SiO_2 core–shell structure have been reported and show enhanced light emission intensity [15–17]. While most previous methods require high-cost precursors, complex equipments and high synthesis temperature. Additionally, these SiC nanostructures are discontinuous and intertwist, which may restrict their optical properties. Therefore, there are numerous challenges in using a feasible method to fabricate SiC nanostructures for practical optical devices.

In this paper, we report a novel and simple method for fabricating hierarchical SiC nanorod arrays by magnetron sputtering using SiO_2 colloidal monolayer spheres as template. The SiC nanorod arrays have a special hierarchical structure with a hexagonal-close-packed arrangement and their improved PL properties are characterized. These results provide insight into the synthesis of SiC nanostructures and may have potential for the design and fabrication of high power electronic devices, light emitting devices, display and related optoelectronic devices.

2. Experimental

SiO_2 colloidal monolayer was fabricated on cleaned Si substrates in a Langmuir–Blodgett trough as described in previous report [18]. Briefly, a droplet of SiO_2 microsphere suspension was cautiously spread on the air–water interface of a Langmuir trough. Then, the SiO_2 film was transferred onto hydrophilic Si substrates. By this way, a close-packed SiO_2 monolayer with controlled sphere diameters (182, 515, 720 and 1500 nm) formed on the substrate.

* Corresponding author. Tel./fax: +86 451 86403767.
E-mail address: yaoli@hit.edu.cn (Y. Li).

0925-8388/$ - see front matter © 2012 Elsevier B.V. All rights reserved.
http://dx.doi.org/10.1016/j.jallcom.2012.05.082

SiC films were deposited onto the colloidal monolayer substrates by radio-frequency (RF) magnetron sputtering method from a SiC target (99.9% purity). The sputtering was performed under the following conditions: an RF power of 140 W, pure Ar atmosphere, and a working pressure of 5 Pa. SiC films were deposited at 250 °C for 3 h. The as-grown SiC films were annealed under N_2 atmosphere for 1 h at 600 °C Other SiC films without SiO_2 monolayer were also achieved for comparison.

The surface morphologies of films were characterized with a Hitachi S-4800 scanning electron microscope (SEM) operating at 30 kV. X-ray diffraction (XRD) pattern was collected using a Cu K_α radiation. The composition and chemical states were examined by X-ray photoelectron spectroscopy (XPS) with a K-Alpha XPS System from Thermo Scientific. PL was measured under the excitation both of Ar^+ laser (488 nm) and Xe lamp (FluoroMax-4 spectrofluorometer) at room temperature.

3. Results and discussion

The morphologies of resulting samples in each step are observed by SEM. Fig. 1a shows the image of SiO_2 colloidal monolayer with sphere size of 515 nm through direct measurement. The monolayer reveals a well-periodic two-dimensional hexagonal close packed (hcp) arrangement. Fig. 1b and Fig. 1c present the top-viewed and cross sectional images of SiC films coated on Si substrates without SiO_2 colloid monolayer template. Dense, smooth and uniform SiC film is prepared and the thickness is around 800 nm. While SiC films on SiO_2 colloid monolayer present the structures of large quantity nanorods as shown in Fig. 1d. An ordered and well-structured array with hcp arrangement SiC nanorods prepares from the pre-existing hcp SiO_2 monolayer. It is demonstrated that SiC nanorods grow vertically on the top of SiO_2 spheres. The diameter of nanorods is almost the same as the spheres. As shown in Fig. 1d, the nanorod arrays have highly rough surfaces which seem to be composed of many nanoparticles. Fig. 1e clearly proves the well-aligned growth of the SiC nanorods. It indicates that each nanorod consists of two parts: one SiO_2 sphere at the bottom and one vertical nanocolumn on the top of the SiO_2 sphere. SiC nanorods are ordered aligned on the spheres and vertical to the spheres plane. The nanorod arrays have a rough arc structure on the surface and the average height of obtained nanorods is about 800 nm. The schematic of formation mechanism of SiC nanorod arrays is shown in Fig. 1f. A dense film will be formed on a bare substrate. If the SiO_2 colloidal monolayer is on the substrate, nanorod arrays will appear due to preferential vertical growth on the direction of the supporting spheres surface. The surface morphologies and the size of SiC nanorods can easily be controlled by the different sizes of SiO_2 spheres.

Fig. 2a shows XRD spectra from SiC nanorod arrays. The feature at $2\theta = 70°$ is from the Si substrate. No intense diffraction peaks of SiC can be observed, suggesting the formation of amorphous SiC. The composition and chemical state of the SiC nanorod arrays are analyzed by XPS. Fig. 2b and c shows the C 1s and Si 2p XPS spectra of the SiC nanorod arrays. The C 1s level spectrum presents two main chemical states: the peak located at 283.1 eV is related to carbon in SiC and the second located at 284.5 eV is attributed to the residual carbon ~284.3 eV for C 1s amorphous graphite [19,20]. The Si 2p peak in Fig. 2b could be decomposed into three peaks, which locate at 99.7, 101.3 and 102.9 eV corresponding to the formation of Si–O, Si–C, C–O–Si in the nanorods. These XPS results indicate the successful formation of SiC.

Different SiC nanorod arrays on SiO_2 monolayer with sphere diameters of 182, 720 and 1500 nm are shown in Fig. 3, respectively. The SEM images present that SiO_2 spheres are densely packed as a hexagonal structure. The defects mainly include single spheres upon the surface of the colloidal crystal, vacancies in the layer and lattice periodicity dislocation. As the diameter of SiO_2 spheres is decreased, the SiC nanorod arrays are more densely integrated and exhibit top aggregation for several neighboring nanorods due to their smaller surface area for SiC nanopartcles agglomerating. It is noticeable that the SiC nanorod arrays prepared from the largest SiO_2 spheres aligned with a short range periodicity because the corresponding SiO_2 monolayer possesses more defects and has only a shorter range ordering (Fig. 3c and e).

The PL intensities of SiO_2 colloidal monolayer, SiC films and SiC nanorod arrays under room temperature are shown in Fig. 4. It can be seen that SiO_2 colloidal monolayer and SiC films have a weak emission band located mainly in the red region. Zhou and Xu have reported a similar emission spectrum from SiC and the origin of the PL is attributed to the vacancy and surface states [13,21]. From the comparison, it is obvious that the PL intensities of SiC nanorod arrays increase, accompanying with five characteristic emission centers. The peak at 693.5 and 766.9 nm may be related to the interface of SiC and SiO_2. The stronger wave packs at about 609.5, 723.1 and 825.8 nm are attributed to the band-gap and

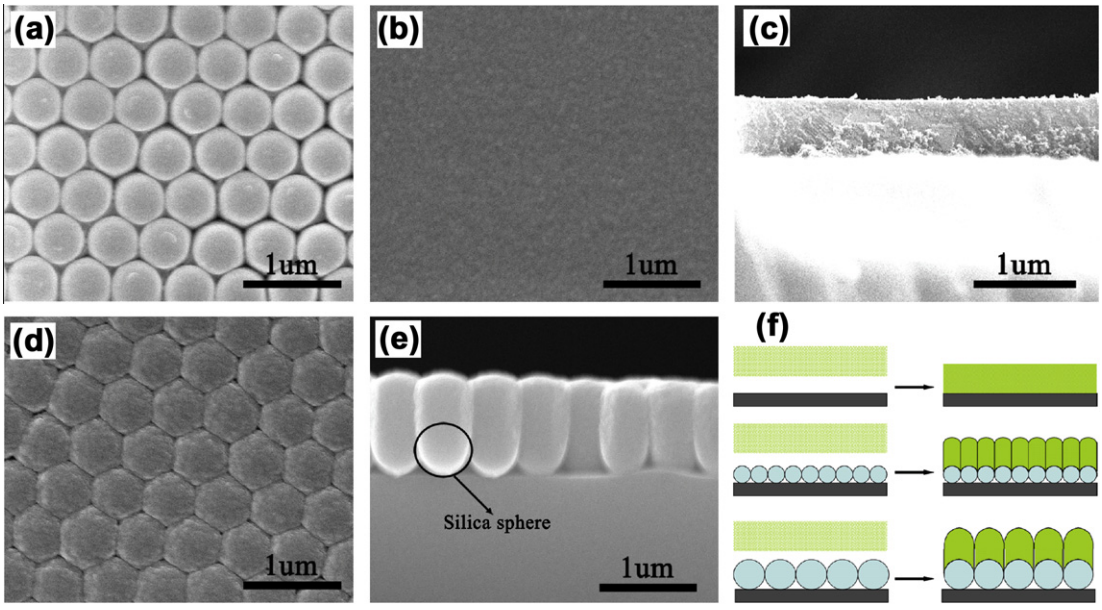

Fig. 1. SEM images of (a) is SiO_2 colloidal monolayer, (b) and (c) are top-viewed and cross sectional images of SiC films; (d) and (e) are top-viewed and cross sectional images of SiC nanorod arrays; (f) schematic of formation mechanism of SiC nanorod arrays.

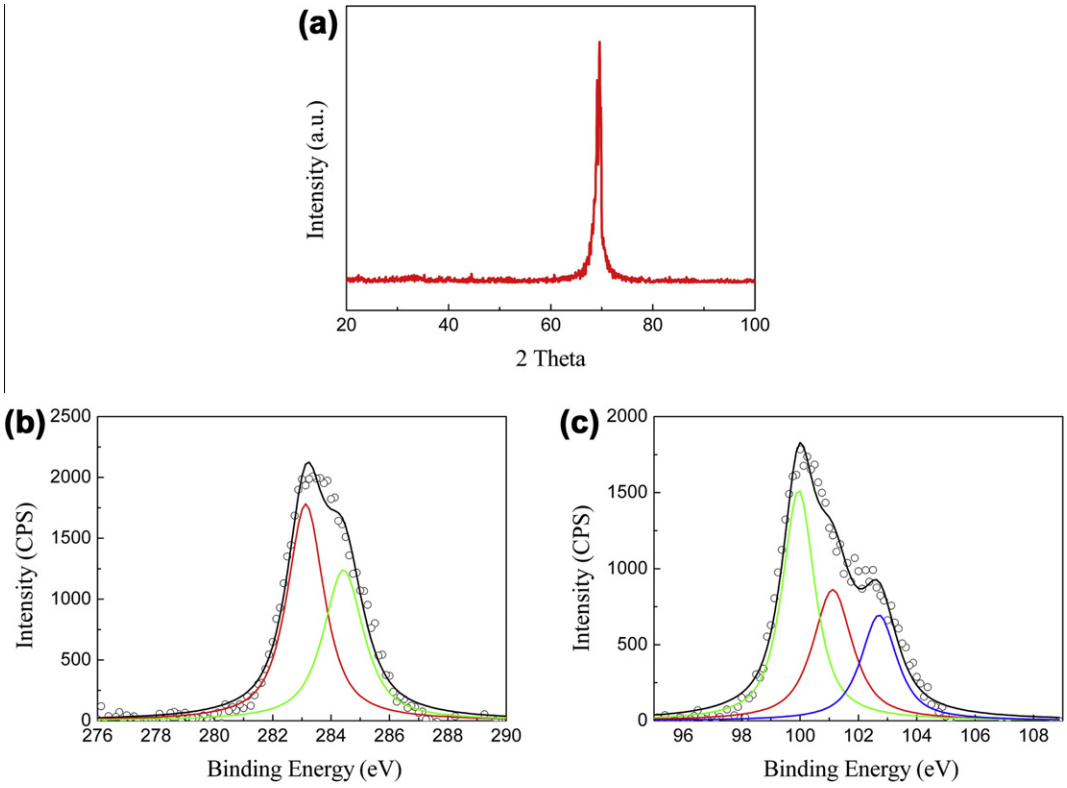

Fig. 2. XRD pattern of (a), XPS spectra of (b) C 1s and (c) Si 2p of SiC nanorod arrays.

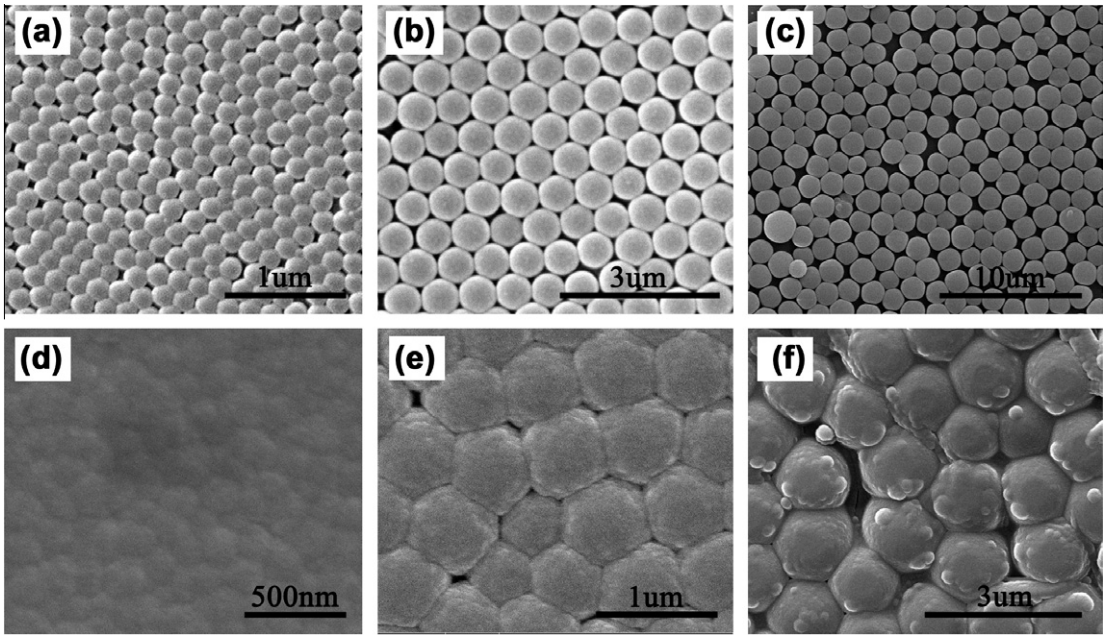

Fig. 3. SEM images of SiO_2 colloidal monolayer and the corresponding SiC nanorod arrays with different diameters: 182 nm for (a) and (d); 720 nm for (b) and (e); 1500 nm for (c) and (f).

defect-related emissions of SiC. Fig. 4b shows the comparison of normalized integrated intensity, which exhibits that SiC nanorod arrays reveal enhanced emission up to 4.3 times. The improved PL performance of SiC nanorod arrays may be provided by the special light manipulating properties of nanorod structures [22]. The group velocity of photons in the nanorod arrays may be slowed down and increase the density of optical states. The interaction of light with the periodic SiC nanorod arrays can be enhanced. Accordingly, the two dimensional periodic nanorod arrays can modify the light propagation and the emission properties. The

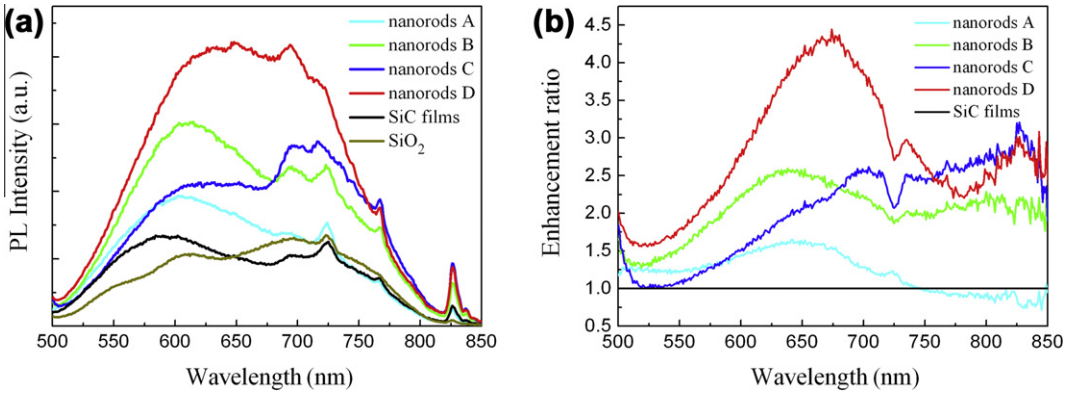

Fig. 4. (a) PL spectra of SiO_2 colloidal monolayer, SiC films, nanorod arrays A, B, C, D, with sphere size of 182, 515, 720 and 1500 nm, respectively; (b) calculated PL enhancement ratios with intensities normalized with the SiC films.

optical gain of SiC nanorod arrays indicates an obvious PL enhancement. Extra enhancement also can be probably due to the greater surface area of the nanorod arrays structure.

As can be seen in Fig. 4, the diameter of SiC nanorods plays an important rule in the PL peak intensity. With the increase of sphere size from 182 to 1500 nm, the PL intensity is trebled. The results suggest that diameters and morphologies of nanorods may affect their luminescence characteristics. Kim has reported similar experimental results of ZnO with the increase of nanorod's diameters [23]. Additionally, the sample D has a rough and large surface area that can improve the efficiency of light emission. Wang et al. have reported on an enhanced PL from different morphologies [24–27]. Therefore, it is reasonably believed that the dependence of PL performance on the diameter of nanorods is attributed to the size effect and surface morphologies. Fig. 4 also show that the PL peak shifts in different SiC nanorod arrays. The shift of the PL peak is attributed to the light emission from the top and the side surfaces of the nanorods with different diameters [28]. The shift can also be caused by the light extraction efficiency that affected by the disorder and defect present in the nanorod arrays.

4. Conclusions

In summary, periodic SiC nanorod arrays are fabricated through magnetron sputtering process by utilizing SiO_2 colloidal monolayer as template. Results show that SiC particles grow vertically on the SiO_2 spheres monolayer and the size of spheres can affect the morphologies of nanorod arrays. The arrays prepared from smaller SiO_2 spheres are prone to be densely integrated and top aggregation; while from the bigger spheres have a shorter periodicity. As shown by the SEM observation of morphological evolution and the corresponding photoluminescence results, the nanorod arrays with a two dimensional periodic arrangement exhibit enhanced photoluminescence properties due to the nanoscale spatial effect on special light manipulating properties and greater surface areas. The parameter- photoluminescence results demonstrate that the photoluminescence enhancement ratios are affected by the size of SiC nanorods. This facile fabrication of SiC nanorod arrays with excellent photoluminescence property will greatly extend SiC's applications in display and higher-performance optical devices.

Acknowledgments

We thank National Natural Science Foundation of China (Nos. 51010005, 90916020, 51174063 and 51102068), the Program for New Century Excellent Talents in University (NCET-08-0168), and the Fundamental Research Funds for the Central Universities (HIT.ICRST.2010001) and Sino-German joint project (GZ550).

References

[1] Y. Xia, P. Yang, Y. Sun, Y. Wu, B. Mayers, B. Gates, Y. Yin, F. Kim, H. Yan, Adv. Mater. 15 (2003) 353–389.
[2] Z.L. Wang, ACS Nano. 2 (2008) 1987–1992.
[3] C. Xie, Y. Cui, PNAS 107 (2010) 4489–4490.
[4] T. Ito, S. Okazaki, Nature 406 (2000) 1027–1031.
[5] G.M. Wallraff, W.D. Hinsberg, Chem. Rev. 99 (1999) 1801–1821.
[6] R.D. Piner, J. Zhu, F. Xu, S. Hong, C.A. Mirkin, Science 283 (1999) 661–663.
[7] M. Steinhart, J.H. Wendorff, A. Greiner, R.B. Wehrspohn, K. Nielsch, J. Schilling, J. Choi, U. Gösele, Science 296 (2002) 1997.
[8] M. Steinhart, R.B. Wehrspohn, U. Gösele, J.H. Wendorff, Angew. Chem. Int. Ed. 43 (2004) 1334–1344.
[9] Y.J. Zhang, W. Li, K.J. Chen, J. Alloys Compd. 450 (2008) 512–516.
[10] Y. Li, X.S. Fang, N. Koshizaki, T. Sasaki, L. Li, S.Y. Gao, Y. Shimizu, Y. Bando, D. Golberg, Adv. Funct. Mater. 19 (2009) 2467–2473.
[11] J.H. Zhang, Y.F. Li, X.M. Zhang, B. Yang, Adv. Mater. 22 (2010) 4249–4269.
[12] D.J. Fu, X.R. Zeng, J.Z. Zou, L. Li, X.H. Li, F. Deng, J. Alloys Compd. 486 (2009) 406–409.
[13] J.M. Zhou, H.L. Li, Li Ye, J. Liu, J.X. Wang, T. Zhao, L. Jiang, Y.L. Song, J. Phys. Chem. C 114 (2010) 22303–22308.
[14] Y.G. Xu, M. Guron, X.L. Zhu, L.G. Sneddon, S. Yang, Chem. Mater. 22 (2010) 5957–5963.
[15] L.Z. Cao, H. Jiang, H. Song, Z.M. Li, G.Q. Miao, J. Alloys Compd. 489 (2010) 562–565.
[16] R. Kim, W.P. Qin, G.D. Wei, G.F. Wang, L.L. Wang, D.S. Zhang, K.Z. Zheng, N. Liu, J. Cryst. Growth. 311 (2009) 4301–4305.
[17] B.S. Li, R.B. Wu, Y. Pan, L.L. Wu, G.Y. Yang, J.J. Chen, Q.M. Zhu, J. Alloys Compd. 462 (2008) 446–451.
[18] S. Reculusa, S. Ravaine, Chem. Mater. 15 (2003) 598–605.
[19] Y. Mizokaw, K.M. Gei, C.W. Wilmsen, J. Vac. Sci. Technol. 4 (1986) 1696–1700.
[20] L. Wang, J. Xu, T.F. Ma, W. Li, X.F. Huang, K.J. Chen, J. Alloys Compd. 290 (1999) 273–278.
[21] J. Xu, L. Yang, Y.J. Rui, J.X. Mei, X. Zhang, W. Li, Z.Y. Ma, L. Xu, X.F. Huang, K.J. Chen, Solid State Commun. 133 (2005) 565–568.
[22] C. Wiesmann, K. Bergenek, N. Linder, U.T. Schwarz, Laser Photo. Rev. 3 (2009) 262–286.
[23] Y.S. Kim, S.H. Kang, Acta Mater. 59 (2011) 3024–3031.
[24] S.H. Hu, Y.C. Chen, C.C. Hwang, C.H. Peng, D.C. Gong, J. Alloys Compd. 500 (2010) L17–L21.
[25] D.S. Kang, H.S. Lee, S.K. Han, V. Srivastava, E.S. Babu, S.K. Hong, M.J. Kim, J.H. Song, J.H. Song, H.J. Kim, D.J. Kim, J. Alloys Compd. 509 (2011) 5137–5141.
[26] Q.H. Zhang, J. Wang, C.W. Yeh, W.C. Ke, R.S. Liu, J.K. Tang, M.B. Xie, H.B. Liang, Q. Su, Acta Mater. 58 (2010) 6728–6735.
[27] G.F. Teixeira, M.A. Zaghete, G. Gasparotto, M.G.S. Costa, J.W.M. Espinosa, E. Longo, J.A. Varela, J. Alloys Compd. 512 (2012) 124–127.
[28] K. Kouyama, M. Inoue, Y. Inose, Ni Suzuki, H. Sekiguchi, H. Kunugita, K. Ema, A. Kikuchi, J. Lumin. 128 (2008) 969–971.